



Research Paper

Phytochemical Profiling and GC-MS Analysis of *Annona muricata* Ethanol Leaf Extract as potential agent for Nephrolithiasis management: An *In-vitro* and *In-silico* Investigation

^{1, 3*}Rahman, Samson Adisa; ¹Sulaimon, Lateef Adegboyega; ¹Arogundade, Obafemi Lamiji; and ²Akinolye, Oluseyi Adeboye

¹Department of Chemical Science, College of Natural Science Crescent University, Abeokuta, Ogun State, Nigeria.

²Department of Biochemistry, College of Bioscience, Federal University of Agriculture Abeokuta.

³Department of Veterinary Biochemistry and Pharmacology, College of Veterinary Medicine, Federal University of Agriculture Abeokuta.

*Corresponding author: P.M.B. 2240, Abeokuta, Ogun State

Abstract

Medicinal plants have long been utilized for therapeutic purposes; however, the specific effects and safety profile of ethanol *Annona muricata* leaf extract in nephrolithiasis management remain underexplored. This study aimed to evaluate the phytochemical composition, antioxidant activity, toxicity, and potential molecular mechanisms of the extract in relation to kidney stone formation. Phytochemical profiling was conducted using Gas Chromatography-Mass Spectrometry (GC-MS) and quantitative analysis of active constituents. Antioxidant potential was determined through *in-vitro* assays, including diphenyl-1-picryl-hydrazyl (DPPH) radical scavenging and nitric oxide inhibition, to evaluate its free radical neutralizing capacity. Acute toxicity assessment provided insight into the extract's safety profile and potential therapeutic window. Furthermore, *in-silico* investigations, comprising molecular docking and gene ontology analysis, were employed to elucidate the extract's bioactive interactions at the molecular level, identifying potential mechanisms responsible for its nephroprotective effects. Bioactive compounds identified through GC-MS analysis were found to interact with molecular pathways and gene expressions linked to prevention and inhibition of kidney stone formation. *A. muricata* ethanol extract phytochemicals exhibited the strong binding to TNF- α and IL-1 β with overall binding energy ranges from -3.6 to -6.3 kcal/mol for TNF- α and -4.1 to -5.8 kcal/mol for IL-1 β . Findings from this study provide compelling evidence supporting the therapeutic potential of *A. muricata* in nephrolithiasis prevention and management, highlighting its promise as a natural remedy in kidney stone treatment.

Received 09 July, 2025; Revised 21 July, 2025; Accepted 23 July, 2025 © The author(s) 2025.

Published with open access at www.questjournals.org

I. Introduction

Since antiquity, medicinal plants have been fundamental in healthcare, serving as natural remedies for maintaining wellness, preventing diseases, and facilitating treatment. These plants contain a rich array of bioactive compounds with therapeutic potential, benefiting both human and animal health (Balogun, 2022). Across various traditional medicine systems, including African healing practices, medicinal plants have played an indispensable role (Balogun, 2022). Furthermore, they have significantly contributed to modern pharmacology, leading to the discovery of several pharmaceutical agents derived either directly from natural compounds or through synthetic adaptations of their chemical structures (Aborode et al., 2022).

Compared to synthetic medications, medicinal plants provide distinct advantages such as broader accessibility, affordability, and deep cultural significance in many societies. Their integrative approach to health allows them to target multiple health conditions while typically presenting fewer adverse effects. Despite their numerous benefits, certain challenges persist, including variability in chemical composition, inconsistent

therapeutic efficacy, lack of standardization in processing and regulation, potential toxicity risks, drug interaction concerns, and ecological depletion due to excessive harvesting (Adedeji et al., 2023).

To optimize their contributions to modern medicine, medicinal plants should undergo systematic scientific validation and integration with conventional medical practices. Investigations into their safety and efficacy, identification of active phytochemicals, understanding of their biological mechanisms, improved cultivation techniques, and advancements in drug development based on plant-derived compounds are essential steps. These research efforts ensure that medicinal plants continue to enhance global health both now and in the foreseeable future (Aborode et al., 2022).

The significance of medicinal plants in contemporary healthcare spans multiple areas. From a scientific perspective, their chemical diversity offers promising candidates for drug development and pharmacological research (Balogun, 2022). Culturally, they serve as an enduring link to ancestral knowledge and play a role in preserving indigenous medical traditions (Ogwu & Osawaru, 2022). Socially, they contribute to accessible healthcare solutions for underprivileged communities, offering cost-effective alternatives to mainstream treatments (Afolabi, 2013). Ecologically, the conservation of medicinal flora supports biodiversity preservation and promotes sustainable environmental practices (Ogwu & Osawaru, 2022).

The therapeutic efficacy of medicinal plants is attributed to their bioactive compounds, commonly referred to as phytochemicals. These compounds encompass diverse classes, including phenolics, flavonoids, terpenoids, alkaloids, saponins, tannins, glycosides, and steroids, each demonstrating distinct structural and functional properties (Isaac et al., 2022). Phenolics and flavonoids are widely recognized for their antioxidant and anti-inflammatory activities, terpenoids and alkaloids exhibit anticancer and antidiabetic effects, while saponins and tannins possess antimicrobial and antiparasitic capabilities. Additionally, glycosides and steroids contribute to cardiovascular regulation and hormonal balance (Olugbuyi et al., 2023). These phytochemicals form the foundation of plant-based medicine, reinforcing their potential in therapeutic applications.

Extensive phytochemical analyses of various parts of *Annona muricata* have uncovered a diverse range of bioactive constituents, including alkaloids, megastigmanes, flavonol triglycosides, phenolic compounds, cyclopeptides, essential oils, and annonaceous acetogenins (Mutakin et al., 2022). Additionally, *Annona muricata* is rich in essential minerals such as potassium, calcium, sodium, copper, iron, and magnesium, highlighting its nutritional benefits and potential physiological contributions to human health (Olugbuyi et al., 2023).

This research seeks to examine the qualitative and quantitative phytochemical composition of *Annona muricata* ethanol leaf extract, assess its *in-vitro* antioxidant and antiradical properties, and perform *in-silico* screening of its bioactive constituents utilizing GC-MS analysis. Furthermore, the study aims to evaluate the extract's toxicological profile (LD₅₀) to establish its safety and suitability for therapeutic applications.

II. Materials and Methods

Chemicals and Reagents

The chemicals and reagents used in this study were obtained in high-purity and analytical-grade form from Sigma Chemical Company Ltd, UK, and British Drug House (BDH) Chemical Ltd, UK.

Collection of Plant Sample

Mature and healthy leaves of *Annona muricata* were harvested from a private residence in the Eleweeran area of Abeokuta. To confirm the plant's identity, a botanist from the Department of Pure and Applied Botany at the Federal University of Agriculture, Abeokuta, Nigeria, authenticated the specimen and assigned it the herbarium number FHA 4549.

Preparation of *Annona muricata* leaves Sample

The collected leaves were carefully washed to eliminate any contaminants before being transferred to the laboratory. They were then systematically arranged on a clean, sterile surface and left to undergo an air-drying process for around six weeks. After achieving complete dryness, the leaves were finely milled into powder and securely stored in an airtight container for future applications.

Preparation of *Annona muricata* leaves ethanol extract

The ethanol-based extraction of *Annona muricata* leaves followed the method outlined by (Nafiu & Ogunsola, 2023). A total of 200g of finely powdered leaves was immersed in 1L of ethanol within a sterile beaker. The solution was maintained at room temperature and allowed to stand for twelve hours, with occasional gentle stirring to enhance extraction. Afterward, the mixture underwent filtration using clean cotton wool and Whatman filter paper No. 1 to remove solid residues. The ethanol solvent was then eliminated through rotary evaporation, yielding a concentrated semi-solid extract. This extract was carefully transferred into a clean glass container and stored in a refrigerator to ensure its stability for future applications.

Qualitative phytochemical Analysis of *Annona muricata* leaves ethanol extract

The Phytochemical screening of the presence of saponins (indicated by stable froth and olive oil emulsion), flavonoids (yellow coloration), tannins (brownish-green color), alkaloids (turbidity with Dragendorff's reagent),

glycosides (brown ring), steroids (red chloroform layers), phlobatannins (red precipitate), anthraquinones (pink ammoniacal phase coloration), terpenoids (reddish-brown interface coloration), reducing sugars (brick-red precipitate via Benedict's test), and phenols (deep violet-purple coloration) (Ajiboye & Olawoyin, 2020; Khanal, 2021).

Quantitative phytochemical Analysis of *Annona muricata* leaves ethanol extract

Quantitative analyses were performed to determine the content of flavonoids, alkaloids, saponins, terpenoids as described by Khanal (2021), and phenols along with reducing sugars (Ajiboye & Olawoyin, 2020).

GC-MS Analysis of *Annona muricata* leaves ethanol extract

GC-MS analysis of the ethanol leaf extract was conducted on a Shimadzu GC-MS Qp2010 Ultra system equipped with an OPTIMA-5-MS capillary column, utilizing a helium carrier gas, split injection, a temperature program from 60°C to 290°C, and a mass spectrometer scanning 30–300 m/z at 70 eV, with compound identification performed against the NIST MS search 2.0 library (Hassan et al., 2020).

Antioxidant Activity of *Annona muricata* leaves ethanol extract

Annona muricata leaves ethanol extract's antioxidant capacity was determined using the DPPH method, measuring the decrease in absorbance at 516 nm after 10 minutes to calculate the IC₅₀ value (based on an absorbance change of 0.4 and an ascorbic acid standard at 29 mM) (Ursini et al., 1994). And the extract nitric oxide scavenging potential was assessed by incubating the extract with 10 mM sodium nitroprusside in phosphate buffer, followed by the addition of Griess reagent, with absorbance measurement at 540 nm to determine the percentage inhibition (Khanal, 2021; Udofia et al., 2022).

In-Silico Analysis of Antinephrolithiasis Properties (Pathways and gene ontology analyses)

To explore the protective potential of *Annona muricata* ethanol extracts against calcium oxalate (CaOx) nephrolithiasis, bioactive compounds identified via GC-MS were compiled into a database; their SMILES representations, retrieved from PUBCHEM (Kim et al., 2016) and CAS Common Chemistry (Schulz & Georgy, 2012), were then used with the Swiss Target Prediction tool (Gfeller et al., 2014) to predict their biological targets in *Mus musculus*.

In-Silico Analysis of anti-inflammatory properties (Molecular Docking)

The three-dimensional (3D) structures of the molecular targets TNF- α (PDB ID: 2AZ5) and IL-1 β (PDB ID: 8C3U) were retrieved from the Protein Data Bank (www.rcsb.org), processed using Chimera 1.12 (ligand/water removal, hydrogen addition, energy minimization (Wang et al., 2006)), and then used as targets for molecular docking with GC-MS identified compounds (ligands) obtained in SDF format from PubChem; ligand binding affinities were assessed using Auto Dock Vina from PyRx (Kumar et al., 2021), and molecular interactions visualized with Discovery Studio 2020.

In-silico pharmacokinetics prediction and drug likeness test

The adsorption, distribution, metabolism, excretion (ADME), and drug-likeness of the phytochemicals were determined using the SWISS ADME and admet SAR webserver (Cheng et al., 2014).

Acute Toxicity Study (Lethal dose LD₅₀) of the of *Annona muricata* leaves ethanol extract

Acute (24 hours) toxicity test of the extract was carried out according to the method described by (Akinloye & Ugbaja, 2022). This method made use of nine rats divided into three groups (n=3) of respective doses of the extract (1500, 3000, and 6000 mg/kg body weight). The first stage involved the administration of 1500mg/kg body weight, and when no sign of toxicity or abnormal behaviour was seen, then 3000mg/kg body weight (second stage) of the extract was given to another group of rats. Finally, when no sign of toxicity or abnormal behaviour was observed, the last administration of 6000mg/kg body weight of the extract was carried out. All the animals were then observed further for 24 hours to note any physiological alterations such as fur texture, locomotion, respiratory rhythm, and any other health indicator or death.

Statistical Analysis

Data are presented as the mean \pm standard error of the mean (SEM), and were analyzed using one-way analysis of variance (ANOVA) followed by Duncan's post hoc test for multiple comparisons in SPSS version 20.0, with p<0.05 considered statistically significant.

III. Results

The quantitative and qualitative phytochemical screening test results of the extract in tables 1 and 2, respectively. Tannin was found to be the highest (101.85mg/100g) while anthraquinone was the least (11.615 mg/100g).

The GC-MS spectrum confirmed the presence of various components with different retention times showing 26 peaks (Figure 1). These compounds were identified through mass spectrometry attached with GC. The major phytochemical constituent's mass spectra and being the most abundant one is shown in table 3.

In-vitro Antioxidant screening result of *Annona muricata* ethanol leaf extracts

Figure 2 shows the stable 1, 1- diphenyl-2-picrylhydrazyl DPPH's radical scavenging activity of *A. muricata* ethanol extract. The inhibition potentials of the extract increase in a concentration dependent manner with 100 µg/ml having higher inhibition potential than that of the standard (Butylated hydroxytoluene-BTH). The IC₅₀ of *A. muricata* ethanol extract is 64.48 µg/ml and that of the standard is 42.51 µg/ml.

Figure 3 shows the antioxidant activity of *A. muricata* ethanol extract. The nitric oxide's radical scavenging ability of the extract was concentration dependent, at higher concentration the scavenging capacity of *A. muricata* ethanol extract is high. The IC₅₀ of the extract is 54.77 µg/ml and that of the standard is 20.60 µg/ml.

Table 1: Qualitative phytochemical screening test result of *A. muricata* ethanol extract

S/N	Phytochemical screened	Result of the test
1	Tannin	+
2	Phenol	+
3	Phlobatannin	+
4	Alkaloid	+
5	Saponin	+
6	Flavonoid	+
7	Steroid	+
8	Anthraquinone	+
9	Terpenoid	+
10	Glycosides	+
11	Reducing sugar	+

Note: + = positive, which means present.

Table 2: Quantitative phytochemical screening test result of *A. muricata* ethanol extract

S/N	Phytochemical Tested	Concentration (mg/100g)
1	Tannin	101.85 ± 0.38
2	Phenol	51.305 ± 0.095
3	Saponin	83.975 ± 0.175
4	Alkaloid	49.22 ± 0.26
5	Reducing sugar	56.52 ± 0.13
6	Glycoside	20.455 ± 2.145
7	Anthraquinone	11.615 ± 0.055
8	Flavonoid	41.92 ± 0.26
9	Terpenoid	18.75 ± 0.2

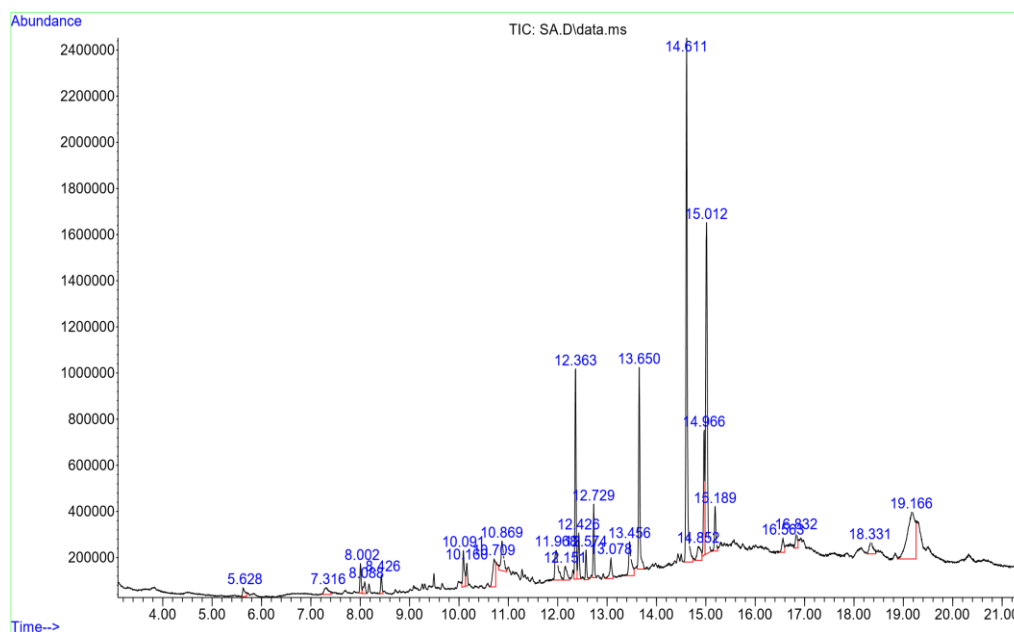
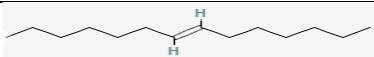
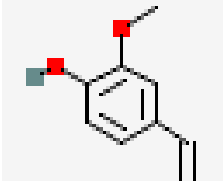

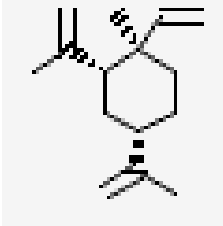
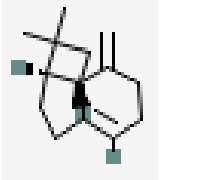

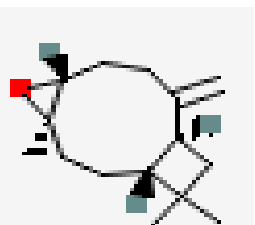




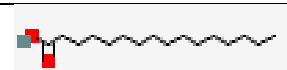
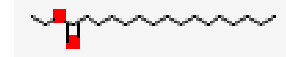

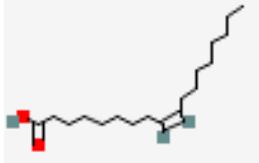

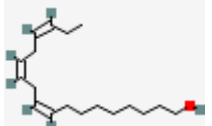
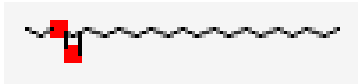



Figure 1: GC-MS of the *Annona muricata* leaf ethanol extract

Table 3: Compounds identified by GC/MS of *A. muricata* leaf ethanol extract

S/N	Peak	RT	Area %	Name of compound	Molecular formula	Structure
1	1	5.628	0.63	7-Tetradecene, (Z)-	C ₁₄ H ₂₈	
2	2	7.316	0.94	2-Methoxy-4-vinylphenol	C ₉ H ₁₀ O ₂	
3	3	8.002	1.12	4-Tetradecene, (E)-	C ₁₄ H ₂₈	
4	4	8.088	0.73	Cyclohexane, 1-ethenyl-1-methyl-2, 68844 000515-13-9 74 4-bis(1-methylethenyl)-, [1S-(1.alpha.,2.beta.,4.beta.)]-	C ₁₅ H ₂₄	
5	5	8.426	0.75	Caryophyllene	C ₁₅ H ₂₄	
6	6	10.091	1.75	1-Nonadecene	C ₁₉ H ₃₈	
7	7	10.160	0.92	Caryophyllene oxide	C ₁₅ H ₂₄ O	
8	12	12.363	7.31	Neophytadiene	C ₂₀ H ₃₈	
9	13	12.426	1.94	Carbonic acid, prop-1-en-2-yl tetradecyl ester	C ₁₈ H ₃₄ O ₃	
10	14	12.574	1.11	3-Eicosyne	C ₂₀ H ₃₈	
11	16	13.078	1.22	5,9,13-Pentadecatrien-2-one, 6,10, 14-trimethyl-	C ₁₈ H ₃₀ O	

S/N	Peak	RT	Area %	Name of compound	Molecular formula	Structure
12	17	13.456	2.70	n-Hexadecanoic acid	C ₁₆ H ₃₂ O ₂	
13	18	13.650	7.84	Hexadecanoic acid, ethyl ester	C ₁₈ H ₃₆ O ₂	

14	19	14.611	20.79	Phytol	C ₂₀ H ₄₀ O	
15	20	14.852	1.61	Oleic Acid	C ₁₈ H ₃₄ O ₂	
16	21	14.966	4.98	Linoleic acid ethyl ester	C ₂₀ H ₃₆ O ₂	
17	22	15.012	16.17	9,12,15-Octadecatrien-1-ol, (Z,Z,Z)-	C ₁₈ H ₃₂ O	
18	23	15.189	1.89	Octadecanoic acid, ethyl ester	C ₂₀ H ₄₀ O ₂	
19	25	16.832	0.94	1,6,10,14,18,22-Tetracosahexaen-3-ol, 2,6,10,15,19,23-hexamethyl-, (all-E)-(.+/-.-)-		
20	26	18.331	1.3	2(1H)-Naphthalenone, octahydro-4a-methyl-7-(1-methylethyl)-, (4a.alpha.,7.beta.,8a.beta.)-	C ₁₄ H ₂₄ O	
21	27	19.166	11.18	Heptadecane	C ₁₇ H ₃₆	

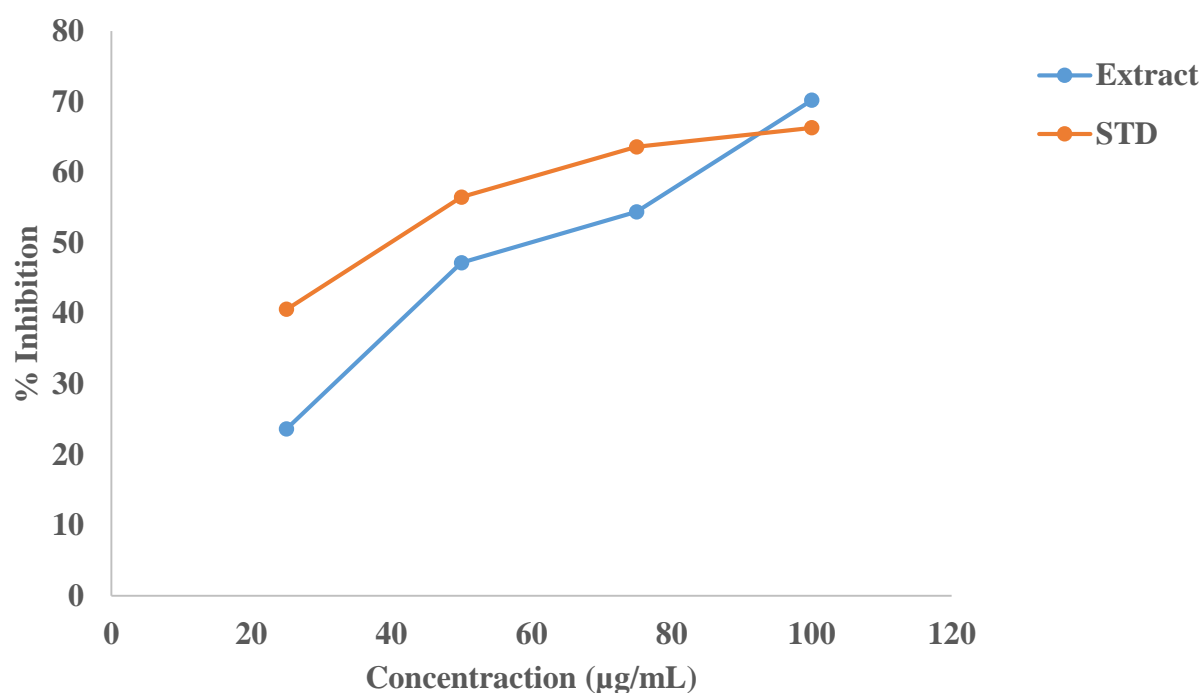


Figure 2: Graph comparing the DPPH's radical scavenging activity of different concentrations of BHT (STD) and *A. muricata* leaf ethanol extract. Values are expressed as mean \pm SEM.

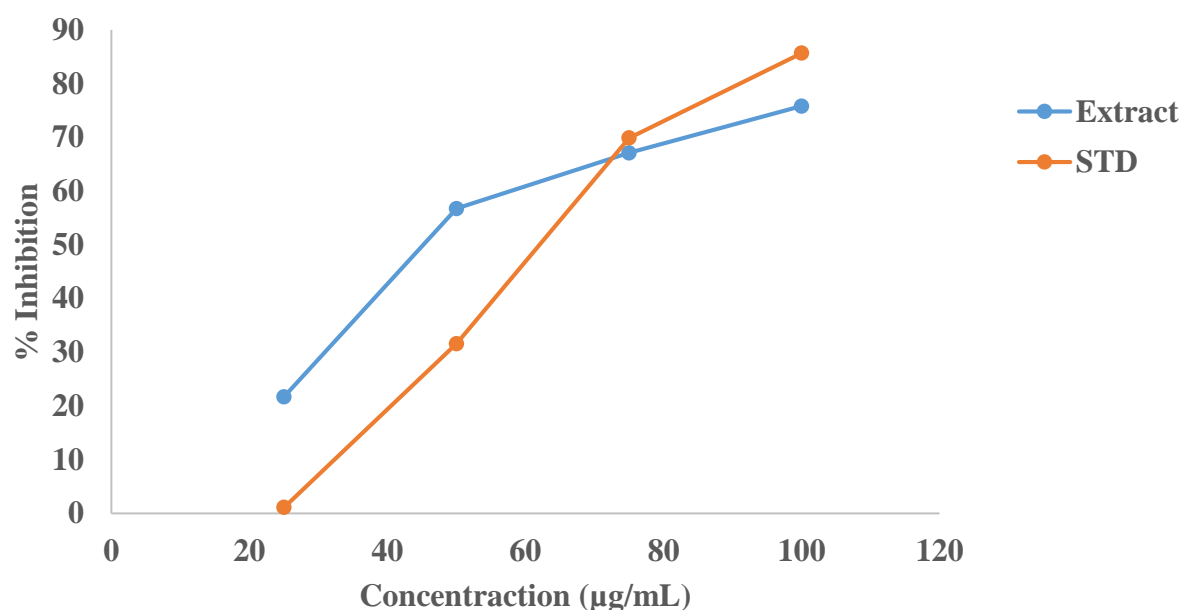


Figure 3: Graph comparing the Nitric oxide's radical scavenging activity of different concentrations of Ascorbic acid (STD) and *A. muricata* leaf ethanol extract. Values are expressed as mean \pm SEM.

Pathway and gene ontology analysis of *A. muricata* biotargets

A total of 277 targets were obtained for the ethanol extract of *A. muricata* (probability score ≥ 0.1), from the Swisstarget prediction software based on the GCMS analysis of *A. muricata* leaf ethanol extract. The intersection of these targets with curated nephrolithiasis targets from the Genecard database and those from the RNA-seq dataset (GSE208528) identified 134 biotargets (adjusted p-value ≤ 0.05 ; logFC ≥ 1.5) OTs, 68 of which were up-regulated and 66 down-regulated, as shown in Table 4. Using the MCODE App of the Cytoscape software to cluster the PPI network of the OTs, 11 targets were highlighted as hub genes mediating the protective effects of *A. muricata* phytochemicals (bioactives) against calcium oxalate nephrolithiasis (Figure 4). These included Collagen Type I Alpha 1 Chain (COL1A1), Collagen Type III Alpha 1 Chain (COL3A1), Secreted Protein Acidic and Cysteine Rich (SPARC), Collagen Type I Alpha 2 Chain (COL1A2), Collagen Type IV Alpha 1 Chain (COL4A1), Biglycan (BGN), Fibronectin 1 (FN1), Matrix Gla Protein (MGP), TIMP Metalloproteinase Inhibitor 1 (TIMP1), Secreted Phosphoprotein 1 (SPP1), and Epidermal Growth Factor (EGF). Pathway enrichment analysis using the Enrichr tool identified that *A. muricata* bioactives significantly impacted several key pathways, including extracellular matrix organization, collagen biosynthesis and modifying enzymes, collagen formation, ECM proteoglycans, ECM-receptor interaction, focal adhesion, and PI3K-Akt signaling pathway (Figure 5). Interestingly, *A. muricata* bioactives impacted significantly several biological processes, cellular components and molecular function gene ontology terms. This was indicated by the significant enrichment of GO terms associated with collagen fibril organization (GO: 0030235), extracellular matrix organization (GO: 0030198), cell-matrix adhesion (GO: 0007160), regulation of calcium ion transport (GO: 0006816), regulation of integrin-mediated signaling pathway (GO: 1903031), collagen-containing extracellular matrix (GO: 0030020), and basement membrane (GO: 0005604) (Figure 6).

Table4: Differentially Expressed *A. muricata* Biotargets in CaOx Nephrolithiasis (logFC > 1.5)

GeneID	baseMean	log2FoldChange	lfcSE	stat	pvalue	padj
Havr1	183.1117	9.55	1.504373	6.34816	2.18E-10	1.18E-07
Timp1	24.50246	8.092179	1.674356	4.83301	1.34E-06	0.000197
Lcn2	43.78689	5.879103	1.043803	5.632389	1.78E-08	4.51E-06
C3	51.34266	5.689351	0.90515	6.285536	3.27E-10	1.38E-07
Aldh1a2	15.52473	4.94506	1.330538	3.716587	0.000202	0.009723
Lyz2	171.5767	4.818923	0.730704	6.5949	4.26E-11	4.05E-08
Sprr1a	64.0902	4.813687	0.72039	6.682056	2.36E-11	2.99E-08
Col1a1	36.94942	4.5989	0.970855	4.73696	2.17E-06	0.000275

Spp1	3313.895	4.57393	0.43603	10.48995	9.61E-26	3.65E-22
S100a6	46.03525	4.493582	0.808245	5.559677	2.70E-08	6.05E-06
Col3a1	35.13962	4.289384	0.923963	4.642377	3.44E-06	0.000374
Fgg	19.25443	4.227232	1.021897	4.136652	3.52E-05	0.002537
Fn1	14.25749	4.205083	1.251025	3.361311	0.000776	0.026114
Anxa3	21.86471	4.07911	0.996798	4.092211	4.27E-05	0.002852
Cp	19.79463	3.926883	0.975117	4.027089	5.65E-05	0.003522
Col1a2	19.59762	3.910968	1.07649	3.633073	0.00028	0.012534
Hspb1	74.75487	3.837548	0.686493	5.590078	2.27E-08	5.40E-06
C1qc	22.39455	3.83445	1.019016	3.762896	0.000168	0.008521
Ctss	33.58664	3.834059	0.889398	4.310849	1.63E-05	0.001289
Mgp	187.7851	3.725066	0.657699	5.663785	1.48E-08	4.02E-06
Cyr61	75.30137	3.705936	0.587516	6.307804	2.83E-10	1.35E-07
C1qb	54.68687	3.699727	0.770877	4.799376	1.59E-06	0.000216
Arg2	13.42428	3.672916	1.098992	3.342078	0.000832	0.027506
Gdf15	29.94614	3.658405	0.807954	4.527988	5.95E-06	0.000596
C1qa	42.99512	3.647456	0.834029	4.373295	1.22E-05	0.001083
Fcer1g	19.33261	3.606076	1.045842	3.448013	0.000565	0.021654
Tyrobp	18.30129	3.523156	1.032916	3.410884	0.000648	0.023459
Cd14	15.23971	3.520472	1.069201	3.29262	0.000993	0.030584
Tnfrsf12a	38.99724	3.072204	0.682675	4.500242	6.79E-06	0.000662
Gc	61.79708	3.065634	0.585094	5.239556	1.61E-07	2.78E-05
Gpc3	22.06972	3.00762	0.890484	3.37751	0.000731	0.025527
Apoe	236.1712	2.988601	0.620249	4.818386	1.45E-06	0.000204
Cxcl14	29.68748	2.939559	0.81881	3.590037	0.000331	0.014292
Tmsb10	38.06955	2.935861	0.777674	3.775181	0.00016	0.008332
F2r	29.93395	2.839505	0.814859	3.484658	0.000493	0.019731
Anxa2	37.51626	2.8241	0.728573	3.876209	0.000106	0.006024
Cyp4a14	47.55261	2.762231	0.802978	3.439984	0.000582	0.021911
Junb	28.35516	2.753284	0.753655	3.653243	0.000259	0.011938
Acta2	39.05141	2.724954	0.754994	3.609241	0.000307	0.013584
Spns2	39.44707	2.666253	0.647101	4.120307	3.78E-05	0.002617

GeneID	baseMean	log2FoldChange	lfcSE	stat	pvalue	padj
Lgals3	48.2968	2.66185	0.604408	4.40406	1.06E-05	0.000962
Sparc	77.5748	2.636055	0.652779	4.038207	5.39E-05	0.003422
Tubb5	45.27776	2.552447	0.630909	4.045664	5.22E-05	0.003422
Adamts1	25.5195	2.47025	0.750519	3.291387	0.000997	0.030584
Cldn4	23.7657	2.456624	0.777499	3.159648	0.00158	0.043229
Tpm4	72.61342	2.450549	0.580987	4.217904	2.47E-05	0.001876
Nuak2	53.18355	2.387358	0.577221	4.13595	3.53E-05	0.002537
Serping1	36.44058	2.382288	0.710018	3.35525	0.000793	0.026459
Clu	228.2849	2.378183	0.466064	5.102697	3.35E-07	5.54E-05
Bgn	44.51945	2.229383	0.676048	3.297668	0.000975	0.030577
Cd74	230.4169	2.111306	0.550248	3.83701	0.000125	0.006768
Gsta2	130.7645	2.068022	0.467777	4.420959	9.83E-06	0.000912

Tmsb4x	216.5558	1.982309	0.53116	3.732037	0.00019	0.009263
Id3	40.85694	1.96919	0.620759	3.17223	0.001513	0.041699
Rhob	66.64526	1.919659	0.57813	3.320464	0.000899	0.028488
Col4a1	72.17458	1.884619	0.566328	3.327789	0.000875	0.027983
Wfdc2	131.5714	1.882368	0.45334	4.152218	3.29E-05	0.002456
Ifitm3	65.60467	1.859289	0.570713	3.257838	0.001123	0.033364
Cryab	120.6659	1.854985	0.45214	4.102682	4.08E-05	0.002774
Msn	52.9198	1.85394	0.563691	3.288933	0.001006	0.030605
Lad1	54.89134	1.842894	0.548061	3.362571	0.000772	0.026114
Tagln2	88.50243	1.820647	0.517257	3.519813	0.000432	0.017856
Anxa5	103.3404	1.752449	0.515893	3.396923	0.000681	0.024003
Tsc22d1	74.32312	1.745026	0.523822	3.331332	0.000864	0.027983
S100a11	330.2027	1.726738	0.446656	3.865927	0.000111	0.006101
Mt1	98.85595	1.63079	0.473045	3.447428	0.000566	0.021654
Cstb	116.3009	1.538146	0.478458	3.2148	0.001305	0.037335
Adgrg1	123.758	1.536961	0.450513	3.41158	0.000646	0.023459
Ephx2	136.6961	-1.51033	0.44909	-3.36309	0.000771	0.026114
Pah	373.8237	-1.51324	0.479705	-3.15452	0.001608	0.043682
Acox1	260.5555	-1.51848	0.446422	-3.40143	0.00067	0.024003
Slc22a12	489.3774	-1.58079	0.450334	-3.51026	0.000448	0.018311
Cmtm6	105.8282	-1.60753	0.465727	-3.45166	0.000557	0.021654
Acat1	182.682	-1.60874	0.468305	-3.43523	0.000592	0.02208
Ugt3a2	370.6668	-1.6278	0.503349	-3.23393	0.001221	0.035728
Ugt2b38	401.6491	-1.65039	0.462841	-3.56578	0.000363	0.015506
Slc37a4	89.81786	-1.66353	0.508237	-3.27314	0.001064	0.03211
Selenop	621.4438	-1.70113	0.380036	-4.47623	7.60E-06	0.000722
Acadm	204.2785	-1.72683	0.456262	-3.78473	0.000154	0.00813
Csad	69.41531	-1.74207	0.533979	-3.26243	0.001105	0.033086
Kcnj15	134.5093	-1.74522	0.509614	-3.42459	0.000616	0.02274
Slc22a6	258.2121	-1.75532	0.48817	-3.59572	0.000323	0.014144

GeneID	baseMean	log2FoldChange	lfcSE	stat	pvalue	padj
Eci3	114.5955	-1.76296	0.542664	-3.24872	0.001159	0.034185
Crot	91.47657	-1.76534	0.504314	-3.50047	0.000464	0.018795
Pecr	195.1037	-1.77603	0.467763	-3.79686	0.000147	0.007851
Cd36	142.7804	-1.78067	0.487622	-3.65173	0.00026	0.011938
Ace	49.69507	-1.83079	0.584207	-3.1338	0.001726	0.046553
Aadat	112.4213	-1.89561	0.532784	-3.55794	0.000374	0.015799
Atp11a	204.7255	-1.89572	0.43945	-4.31385	1.60E-05	0.001289
Serpinf2	149.196	-1.92048	0.475634	-4.03773	5.40E-05	0.003422
Ces1f	188.4507	-1.93956	0.550192	-3.52524	0.000423	0.017686
Cyp2e1	655.0064	-1.95237	0.586639	-3.32807	0.000875	0.027983
Slc17a3	98.79248	-1.95349	0.519498	-3.76035	0.00017	0.008521
BC024386	93.62472	-1.9763	0.621035	-3.18226	0.001461	0.040873
Mpv17l	163.7536	-1.99053	0.514591	-3.86818	0.00011	0.006101
Aspdh	62.92068	-2.02494	0.595913	-3.39804	0.000679	0.024003

Ehhadh	214.6818	-2.04926	0.511039	-4.00999	6.07E-05	0.003666
Kap	20222.8	-2.10272	0.430873	-4.88013	1.06E-06	0.000161
B4galt5	44.4106	-2.10428	0.608156	-3.4601	0.00054	0.021397
Cyp4b1	1290.823	-2.22792	0.479336	-4.64793	3.35E-06	0.000374
Ubiad1	30.69622	-2.25057	0.682815	-3.29602	0.000981	0.030577
Nudt19	339.4698	-2.2758	0.411115	-5.53568	3.10E-08	6.55E-06
Pank1	83.9277	-2.29628	0.52963	-4.33564	1.45E-05	0.001229
Slc22a30	71.3384	-2.32095	0.621372	-3.73521	0.000188	0.009263
Gm48931	27.47909	-2.32767	0.729306	-3.19162	0.001415	0.039865
Agps	49.52598	-2.35035	0.594881	-3.95095	7.78E-05	0.004627
Acsm2	474.2651	-2.3504	0.467328	-5.02944	4.92E-07	7.80E-05
G6pc	185.9761	-2.3561	0.514497	-4.57942	4.66E-06	0.000479
Slc5a8	60.59178	-2.35915	0.587631	-4.01469	5.95E-05	0.003652
Odc1	515.3724	-2.38341	0.437148	-5.45218	4.98E-08	9.96E-06
Acy3	1354.554	-2.41998	0.44784	-5.40367	6.53E-08	1.24E-05
Fmo5	25.25619	-2.4965	0.773618	-3.22705	0.001251	0.036044
Cyp2a4	130.5388	-2.53378	0.613284	-4.1315	3.60E-05	0.002539
Hsd3b2	37.98888	-2.54014	0.69229	-3.66919	0.000243	0.011427
Slc9a8	31.14024	-2.54055	0.697851	-3.64054	0.000272	0.012321
Mep1b	78.44821	-2.55678	0.587379	-4.35285	1.34E-05	0.001162
Egf	86.81398	-2.61984	0.615487	-4.25654	2.08E-05	0.001612
Slc18a1	34.9795	-2.64743	0.721261	-3.67055	0.000242	0.011427
Amacr	126.4598	-2.68841	0.498301	-5.39516	6.85E-08	1.24E-05
D630029K05Rik	45.58835	-2.70108	0.688626	-3.92242	8.77E-05	0.00513
Lpl	91.69778	-2.70939	0.578174	-4.68612	2.78E-06	0.000321
Slc7a13	325.3696	-2.71651	0.628811	-4.32007	1.56E-05	0.001289
Cyp7b1	79.3677	-2.8149	0.597141	-4.71397	2.43E-06	0.000289
C1qtnf3	56.09632	-2.84767	0.616548	-4.61874	3.86E-06	0.000408

GeneID	baseMean	log2FoldChange	lfcSE	stat	pvalue	padj
mt-Nd4l	230.1936	-2.86082	0.604744	-4.73064	2.24E-06	0.000275
Hsd17b11	114.5662	-2.91033	0.487177	-5.97386	2.32E-09	8.81E-07
Akr1c14	67.03976	-3.02344	0.638945	-4.73193	2.22E-06	0.000275
Inmt	328.262	-3.24115	0.50214	-6.45469	1.08E-10	6.88E-08
Acsm3	109.0296	-3.4084	0.520318	-6.55061	5.73E-11	4.36E-08
Cyp4a12a	83.20731	-3.48002	0.612458	-5.68206	1.33E-08	3.89E-06
Slco1a1	80.04394	-3.67091	0.623503	-5.88755	3.92E-09	1.24E-06
Slc22a7	94.81535	-5.04405	0.651925	-7.73717	1.02E-14	1.93E-11
Angptl7	19.42682	-5.21813	1.339772	-3.89479	9.83E-05	0.005665
Gm6300	47.56252	-5.94256	1.002949	-5.92509	3.12E-09	1.08E-06

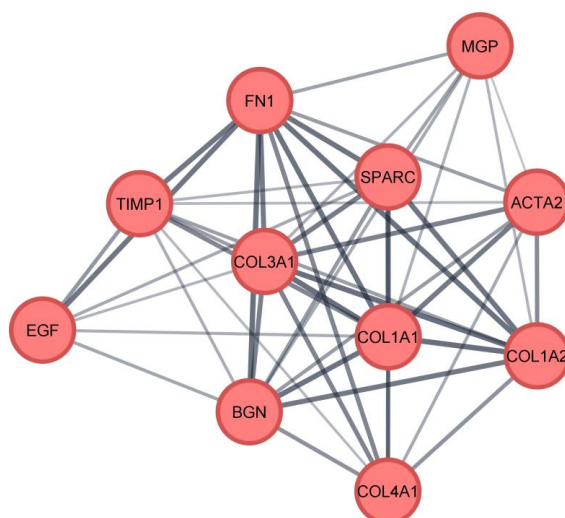


Figure4: MCODE clusters of the PPI network of core targets of ethanol extract *A. muricata* against CaOx Nephrolithiasis.

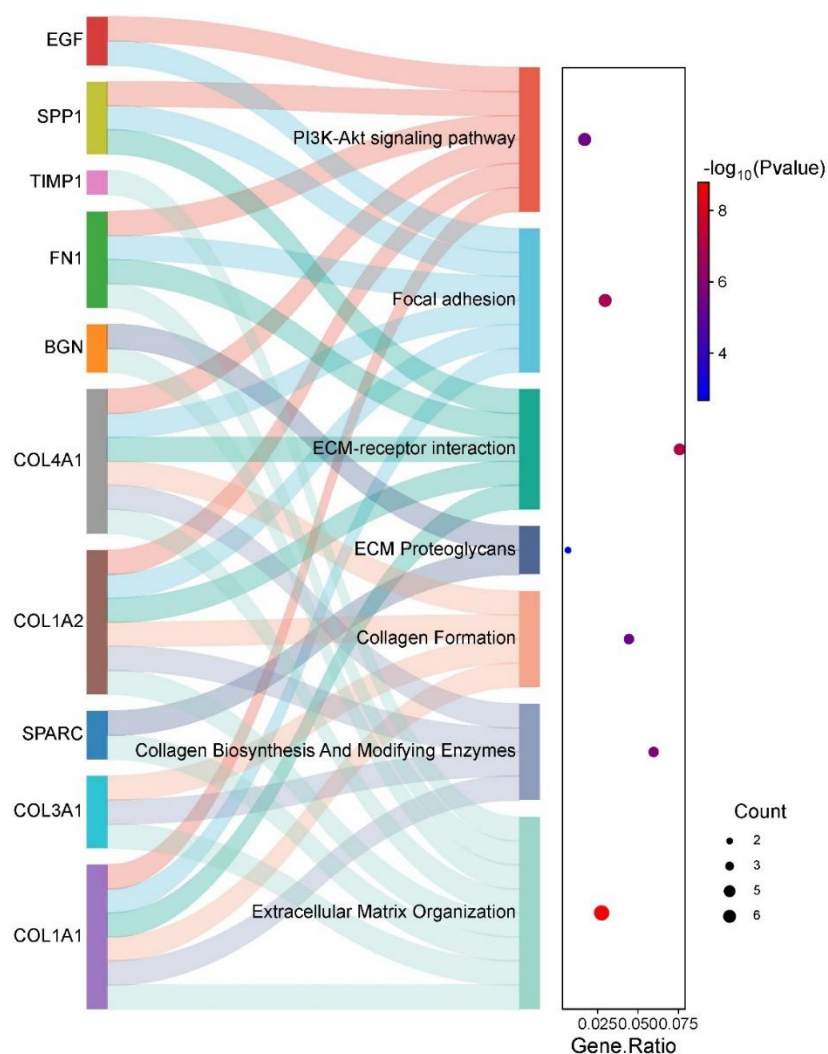


Figure 5: Bubble plot combined with Sankey diagram demonstrating statistically significant KEGG/REACTOME pathways and the genes within each pathway on the y-axis and the gene ratio ($p\text{-value} \leq 0.05$ and $FDR < 0.05$) on the x-axis for the ethanol extract of *A. muricata* against CaOx nephrolithiasis.



Figure 6: Bubble plot demonstrating top enriched GO terms in biological process, cellular component, as well as molecular function on the y-axis and the combined scores of these terms ($p\text{-value} \leq 0.05$ and $FDR < 0.05$) on the x-axis for the ethanol extract of *A. muricata* against CaOx nephrolithiasis.

Molecular docking analysis

A. muricata leaf ethanol extract phytochemical compounds obtained through GC-MS analysis demonstrated varying degrees of binding affinities to both TNF- α and IL-1 β as revealed by the change in Gibbs free energy (ΔG) as shown in Table 5. The binding affinities of standard ligands (compounds 25 and 26) demonstrated strong binding affinities of -6.8 kcal/mol and -9.7 kcal/mol for TNF- α and IL-1 β respectively, serving as reference points for the analysis. Among the test compounds, Caryophyllene oxide (compound 7) exhibited the strongest binding to TNF- α with a binding energy of -6.3 kcal/mol, followed closely by Caryophyllene (compound 5) at -6.1 kcal/mol. For IL-1 β , several compounds showed notable binding affinities of -5.7 kcal/mol, including Caryophyllene oxide, Caryophyllene, and a Cyclohexane derivative (compound 4). The compound 5,9,13-Pentadecatrien-2-one, 6,10,14-trimethyl- (compound 15) demonstrated strong dual-target binding with energies of -5.3 kcal/mol and -5.8 kcal/mol for TNF- α and IL-1 β respectively. Structure-activity relationship analysis (figure 7 and 8) revealed that sesquiterpenes, particularly Caryophyllene and its derivatives, consistently showed strong binding to both targets, while long-chain hydrocarbons generally exhibited weaker interactions ($\Delta G > -4.5$ kcal/mol). The weakest binding was observed with 3(2H)-

Thiophenone, 2-ethylidihydro- (compound 9) for TNF- α (-3.6 kcal/mol) and Octadecanoic acid, ethyl ester (compound 22) for IL-1 β (-4.1 kcal/mol). Overall binding energy ranges for the test compounds were -3.6 to -6.3 kcal/mol for TNF- α and -4.1 to -5.8 kcal/mol for IL-1 β , excluding the standard ligands.

ADME analysis

The ADME (Absorption, Distribution, Metabolism, and Excretion) analysis of 21 compounds revealed diverse pharmacokinetic properties (Table 6). The Consensus Log P values ranged from highly lipophilic compounds like 1-Nonadecene (7.56) to hydrophilic compounds like Methyl-.beta.-D-thiogalactoside (-1.24), with most compounds showing moderate to high lipophilicity. Regarding gastrointestinal (GI) absorption, 13 compounds demonstrated high absorption potential, while 11 showed low absorption, generally correlating with their lipophilicity and molecular size. Blood-Brain Barrier (BBB) permeability was observed in only 7 compounds, including 2-Methoxy-4-vinylphenol, Caryophyllene oxide, 3(2H)-Thiophenone, Ethyl cyclohexanepropionate, Orcinol, n-Hexadecanoic acid, and (E)-pent-2-en-3-yl hexanoate, suggesting potential neurological applications for these compounds. The Topological Polar Surface Area (TPSA) values ranged from 0.00 to 115.45 Å², with Methyl-.beta.-D-thiogalactoside showing the highest TPSA. Solubility classifications varied from "highly soluble" to "poorly soluble," with most compounds falling in the "moderately soluble" category. The bioavailability score was consistent at 0.55 for most compounds, with some exceptions showing higher scores of 0.85 (n-Hexadecanoic acid, Oleic Acid, Linoleic acid ethyl ester, and 9, 12, 15-Octadecatrien-1-ol). Drug-likeness violations were observed in many compounds, with several showing multiple Lipinski rule violations, particularly the long-chain fatty acids and their derivatives. However, seven compounds (2-Methoxy-4-vinylphenol, Caryophyllene oxide, Methyl-.beta.-D-thiogalactoside, 3(2H)-Thiophenone, Ethyl cyclohexanepropionate, Orcinol, and (E)-pent-2-en-3-yl hexanoate) showed no violations.

No mortality was recorded at the dose level of 200-800 mg/kg body weight of the extract over the 24-h period. Furthermore, the animals showed no signs of sedation, aggressiveness, and respiratory distress. Daily observation over the 14 days post-treatment did not show evidence of latent leaf ethanol extract related toxicities.

S/N	Compounds	PubChem ID	ΔG Energy (Kcal/mol)	
			TNF- α	IL1- β
1	7-Tetradecene, (Z)-	5364650	-4.6	-5
2	2-Methoxy-4-vinylphenol	332	-4.9	-5.4
3	4-Tetradecene, (E)-	5364426	-4.1	-4.6
4	Cyclohexane, 1-ethenyl-1-methyl-2,4-bis(1-methylethenyl)-, [1S-(1.alpha.,2.beta.,4.beta.)]-	6431151	-5.0	-5.7
5	Caryophyllene	5281515	-6.1	-5.7
6	1-Nonadecene	29075	-4.2	-4.2
7	Caryophyllene oxide	1742210	-6.3	-5.7
12	Neophytadiene	10446	-4.4	-4.7
13	Carbonic acid, prop-1-en-2-yl tetradecyl ester	91692936	-4.3	-4.6
15	1,4-Eicosadiene	5365774	-4	-4.4
16	5,9,13-Pentadecatrien-2-one, 6,10,14-trimethyl-	61206	-5.3	-5.8
17	n-Hexadecanoic acid	985	-4.2	-4.4

Table 5: Binding free energy values

18	Hexadecanoic acid, ethyl ester	12366	-4.3	-4.4
19	Phytol	5280435	-4.4	-4.8
20	Oleic Acid	445639	-4.2	-4.9
21	Linoleic acid ethyl ester	5282184	-4.3	-4.6
22	9,12,15-Octadecatrien-1-ol, (Z,Z,Z)-	6436081	-4.6	-4.6
23	Octadecanoic acid, ethyl ester	8122	-4	-4.1

S/N	Compounds	PubChem ID	ΔG Energy (Kcal/mol)	
			TNF-α	IL1-β
24	Heptadecane	12398	-3.9	-4.1
25	*6,7-Dimethyl-3-[(methyl2-[methyl(1-[3-(trifluoromethyl)phenyl]-1H-indol-3-YLmethyl)amino]ethylamino)methyl]-4H-chromen-4-one	5327044	-6.8	
26	*(S)-4'-hydroxy-3'-(6-methyl-2-oxo-3-(1H-pyrazol-4-yl)indolin-3-yl)-[1,1'-biphenyl]-2,4-dicarboxylic acid	168477827		-9.7

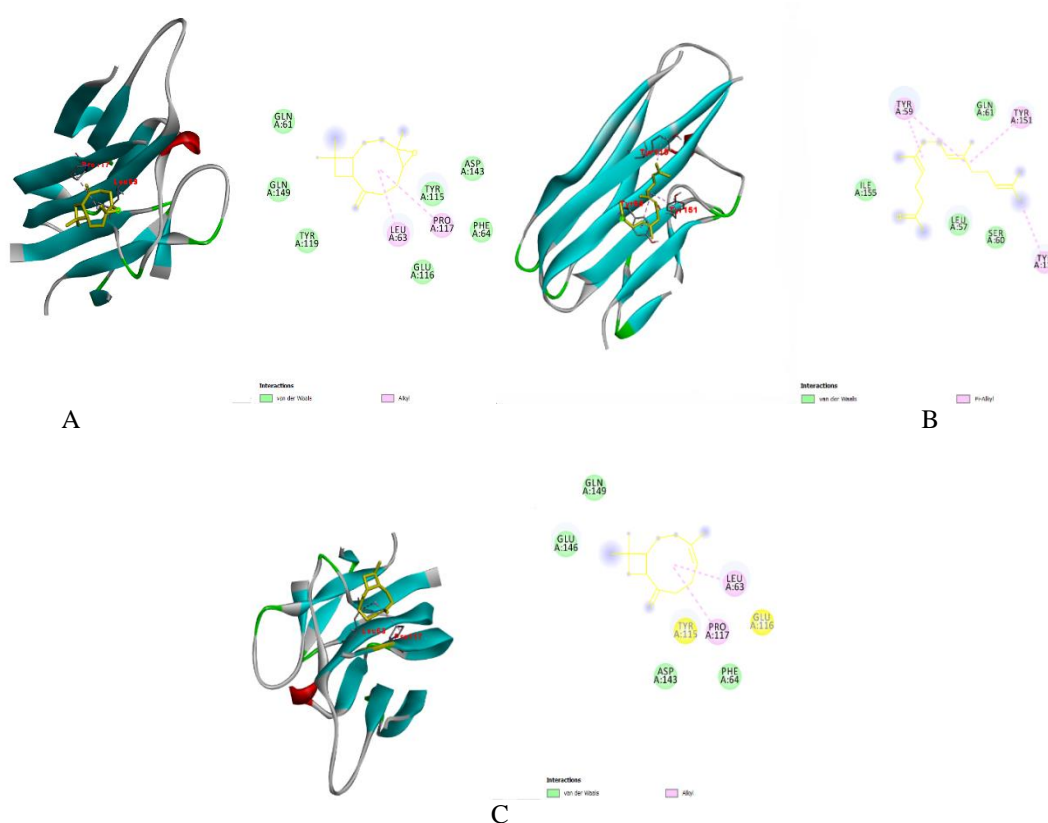


Figure 7: 3D (left) and 2D (right) views of the molecular interactions of amino-acid residues of TNF-α with (A) Caryophyllene oxide (B) 5, 9, 13-Pentadecatrien-2-one, 6, 10, 14-trimethyl- and (C) Caryophyllene

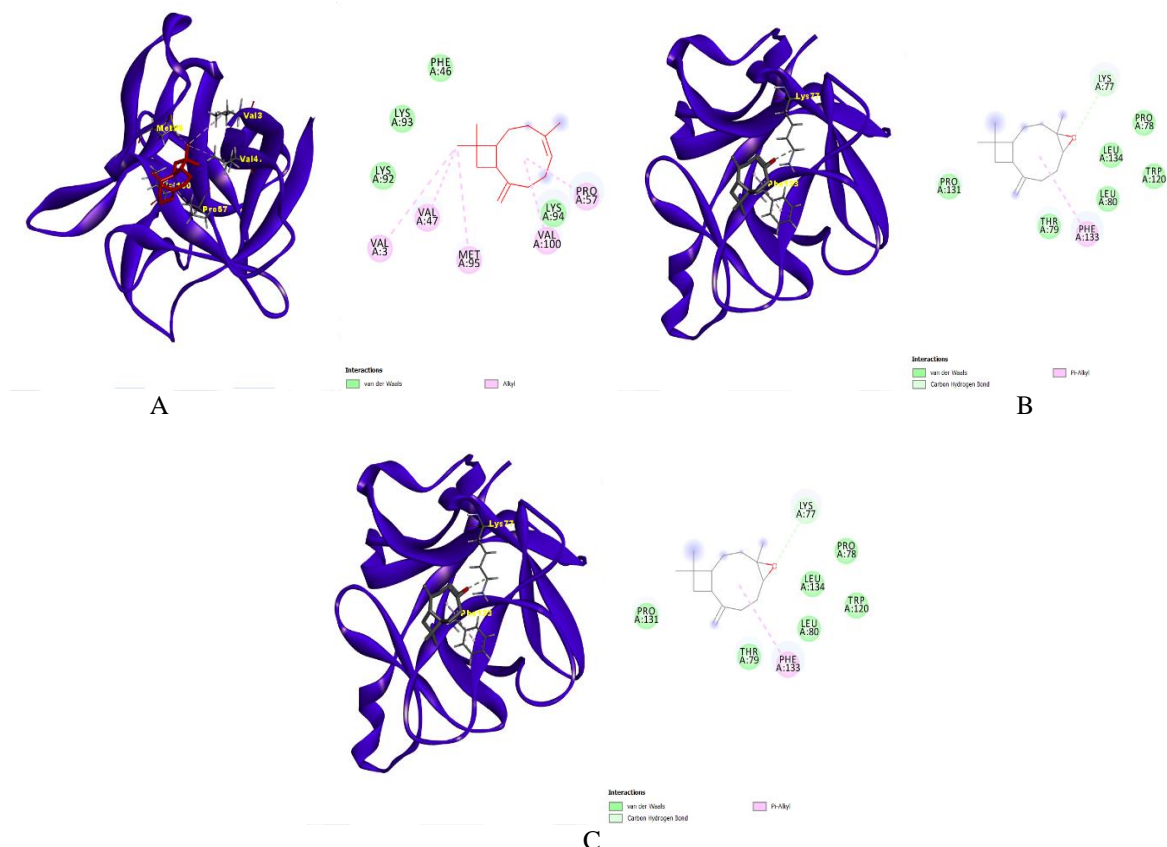


Figure 8: 3D (left) and 2D (right) views of the molecular interactions of amino-acid residues of IL1- β with (A) Caryophyllene (B) Caryophyllene oxide and (C) 5,9,13-Pentadecatrien-2-one, 6,10,14-trimethyl-

Table 6: Drug-likeness

Compounds	Consensus Log P	GI Absorption	BBB Permeant	TPSA	Solubility Class	Bioavailability Score	Drug-likeness Violations
7-Tetradecene, (Z)-	5.48	Low	No	0.00	Moderately soluble	0.55	Lipinski (1)
2-Methoxy-4-vinylphenol	2.14	High	Yes	29.46	Soluble	0.55	None
4-Tetradecene, (E)-	5.48	Low	No	0.00	Moderately soluble	0.55	Lipinski (1)
Cyclohexane, 1-ethenyl-1-methyl-2,4-bis(1-methylethenyl)-, [1S-(1.alpha.,2.beta.,4.beta.)]-	4.63	Low	No	0.00	Moderately soluble	0.55	Lipinski (1)
Caryophyllene	4.24	Low	No	0.00	Soluble	0.55	Lipinski (1)
1-Nonadecene	7.56	Low	No	0.00	Poorly soluble	0.55	Multiple (4)
Caryophyllene oxide	3.68	High	Yes	12.53	Soluble	0.55	None
Methyl-.beta.-D-thiogalactoside	-1.24	High	No	115.45	Highly soluble	0.55	None
3(2H)-Thiophenone, 2-ethylidihydro-	1.53	High	Yes	42.37	Very soluble	0.55	None
Ethyl cyclohexanepropionate	2.96	High	Yes	26.30	Soluble	0.55	None
Orcinol	1.33	High	Yes	40.46	Soluble	0.55	None
Neophytadiene	7.07	Low	No	0.00	Poorly soluble	0.55	Multiple (4)
Carbonic acid, prop-1-en-2-yl tetradecyl ester	5.86	High	No	35.53	Moderately soluble	0.55	Multiple (3)
1,4-Eicosadiene	7.34	Low	No	0.00	Poorly soluble	0.55	Multiple (4)
Compounds	Consensus Log P	GI Absorption	BBB Permeant	TPSA	Solubility Class	Bioavailability Score	Drug-likeness Violations
5,9,13-Pentadecatrien-2-	5.04	High	No	17.07	Moderately	0.55	Multiple (2)

one, 6,10,14-trimethyl-					soluble		
n-Hexadecanoic acid	5.20	High	Yes	37.30	Moderately soluble	0.85	Lipinski (1)
Hexadecanoic acid, ethyl ester	5.90	High	No	26.30	Moderately soluble	0.55	Multiple (4)
Phytol	6.25	Low	No	20.23	Moderately soluble	0.55	Multiple (4)
Oleic Acid	5.65	High	No	37.30	Moderately soluble	0.85	Multiple (4)
Linoleic acid ethyl ester	5.65	High	No	26.30	Moderately soluble	0.85	Multiple (4)
9,12,15-Octadecatrien-1-ol, (Z,Z,Z)-	5.65	High	No	20.23	Moderately soluble	0.85	Multiple (4)
Octadecanoic acid, ethyl ester	6.71	Low	No	26.30	Poorly soluble	0.55	Multiple (4)
(E)-pent-2-en-3-yl hexanoate	3.12	High	Yes	26.30	Soluble	0.55	None
7-Tetradecene, (Z)-	6.79	Low	No	0.00	Moderately soluble	0.55	Multiple (4)

IV. DISCUSSION

This study, conducted using GC-MS analysis and other investigative methods, highlights the antioxidative properties and valuable phytoconstituents of *Annona muricata* leaf ethanol extract, suggesting its potential as a therapeutic agent in disease management. Among the phenolic and flavonoid compounds present, tannin (101.85 ± 0.38) mg/100g exhibited the highest concentration, followed by saponin (83.975 ± 0.175) mg/100g, both of which are known for their health benefits (de Albuquerque et al., 2012). The ethanol extract of *A. muricata*, abundant in bioactive compounds such as terpenoids, polyphenols, and flavonoids, has demonstrated therapeutic potential (Shahzad et al., 2020). Saponins exhibit antiviral and antibacterial properties, while flavonoids are recognized for their anticancer effects. Tannins also contribute to anticancer activity (Shahzad et al., 2020). Additionally, cardiac glycosides support kidney health, phenols possess anti-inflammatory benefits, and steroids aid in reducing inflammation. Terpenoids have been shown to be effective against viral and bacterial infections, as well as conditions such as cancer, malaria, and tuberculosis (Mohammadi-Cheraghbabadi & Hazrati, 2023). Reducing sugars like glucose provide an immediate energy source and are involved in cellular signaling and metabolic pathways (Shehadeh et al., 2021).

The inhibition potentials of *A. muricata* ethanol extract against DPPH radical increase in a concentration dependent manner with 100 µg/ml having higher inhibition potential than that of the standard. DPPH radicals scavenging potentials IC_{50} of *A. muricata* ethanol extract is 64.48 µg/ml and that of the standard is 42.51 µg/ml with differences of 21.97 to that of standard. While nitric oxide's radical scavenging ability IC_{50} of the extract is 54.77 µg/ml compared to 20.60 µg/ml of the standard with differences of 34.17 to that of standard. IC_{50} is a widely used metric for evaluating drug efficacy, reflecting the concentration required to inhibit a biological process by 50% (Akinloye & Ugbaja, 2022). Plant extracts with IC_{50} values between 10–50 mg/mL and closely similar to or possess lower values than standard used are considered potent antioxidants (Akinloye & Ugbaja, 2022; Butnariu et al., 2022). Among the two antioxidant assays performed in this study, the scavenging potential of *A. muricata* ethanol extract against DPPH radical is more pronounced than that of nitric oxide radical, hence indicating the significant anti-oxidative capacity for *A. muricata*, reinforcing its potential medicinal value.

Furthermore, the study examined the protective effects of *A. muricata* ethanol extract against calcium oxalate (CaOx) nephrolithiasis. Bioactive compounds identified through GC-MS analysis were found to interact with molecular pathways and gene expressions linked to kidney stone formation. Lcn2, also known as neutrophil gelatinase-associated lipocalin (NGAL), is recognized as a renal tubular injury marker (Kang et al., 2020). Elevated NGAL levels in a rat model of CaOx kidney stones suggest its involvement in nephrolithiasis pathology through renal injury mechanisms. Additionally, Spp1 encodes osteopontin (OPN), which plays a role in preventing calcium salt precipitation, indicating a potential protective function against stone formation (Arcidiacono et al., 2015). Variations in the FN1 gene have been explored for their potential role in calcium oxalate (CaOx) nephrolithiasis. The study by Onaran et al. (2009) investigated the relationship between FN1 polymorphisms and susceptibility to CaOx kidney stones. A significant link was identified between the HindIII polymorphism of FN1 and an increased risk of stone formation, indicating that genetic variations in this gene may contribute to nephrolithiasis development.

MGP (matrix Gla Protein) has been implicated as a key regulator in nephrolithiasis due to its function as an inhibitor of calcification. Research by Khan (2014) showed that MGP expression is upregulated in renal tubular epithelial cells in response to oxalate and CaOx crystals, suggesting a protective role against stone formation. Elevated MGP levels were also observed in the renal peritubular vessels of hyperoxaluric rats, reinforcing its involvement in stone prevention. Genetic studies have revealed population-specific associations with MGP polymorphisms. Murugesan et al. (2018) identified a significant relationship between SNP rs4236 and nephrolithiasis in the Indian population, while (Keramatipour et al., 2018) reported no such association in Iranian subjects, highlighting possible genetic or ethnic variations in MGP-related susceptibility. Interestingly, Khan (2014) found MGP within Randall's plaques, suggesting a more complex role in stone pathogenesis beyond simple calcification inhibition. Additionally, Sharma and Albig (2013) described MGP's role in angiogenesis, emphasizing its broader biological functions.

ECM organization, involving genes such as COL1A1, COL3A1, SPARC, COL1A2, COL4A1, BGN, FN1, and TIMP1, plays a fundamental role in CaOx nephrolithiasis. These genes encode ECM proteins that contribute to kidney stone formation. Studies indicate that SPARC, a matricellular protein, regulates ECM component expression and participates in collagen processing (McCurdy et al., 2011; Wei et al., 2014). SPARC, along with ECM-related genes such as COL1A1 and FN1, has been linked to cancer progression, tissue remodeling, and pathological calcification (Tian et al., 2022). In nephrolithiasis, ECM components can act as a scaffold for crystal deposition, promoting kidney stone formation. Additionally, ECM disruption affects renal tubular epithelial function, contributing to kidney disease pathology (Sun et al., 2018). Interestingly, ECM-related genes also play a role in oxidative stress responses and renal injury, both of which are crucial in

nephrolithiasis (Kang et al., 2020). Moreover, Randall plaques precursors to CaOx stones have been associated with ECM gene dysregulation and renal dysfunction (Taguchi et al., 2016).

Collagen synthesis, involving COL1A1, COL3A1, COL1A2, and COL4A1, plays a crucial role in CaOx nephrolithiasis. These genes encode essential ECM proteins that contribute to kidney stone formation. Liu et al. (2017) reported that miR-214-5p targets COL4A1, and its inhibition enhances ECM formation in osteoblastic cells, a mechanism potentially relevant to kidney stone pathology. Further supporting this hypothesis, Oefner et al. (2015) identified collagen type IV (COL4A1) as a mediator of trophoblast invasion, a process that might parallel CaOx crystal deposition and retention in renal tubules. AM extract's ability to suppress excessive collagen IV accumulation likely contributed to early inhibition of crystal adhesion and tubular damage (Gross et al., 2010). Focal adhesion molecules regulate cell attachment, migration, and signaling (Chan et al., 2021; Mao et al., 2021). EGF, a ligand for EGFR, is involved in cell proliferation and migration (Song et al., 2013). Given the importance of epithelial integrity and adhesion mechanisms in nephrolithiasis, *A. muricata* ethanol extract phytochemicals appears to modulate focal adhesion pathways, contributing to renal epithelial preservation and reduced crystal attachment sites. This mechanistic insight aligns with previous findings demonstrating EGF-mediated renal healing effects (Chan et al., 2021).

Additionally, EGF signaling influences renal epithelial repair and crystal deposition responses (Pan et al., 2014). The preservation of renal structure and improved urinary parameters noted in this study suggest that *A. muricata* ethanol extract regulates EGF-driven cellular adhesion mechanisms, reinforcing its nephroprotective potential (Song et al., 2013). The PI3K/Akt signaling pathway plays a vital role in cell survival, proliferation, and apoptosis, processes central to calcium oxalate (CaOx) nephrolithiasis pathophysiology (Xu et al., 2024). Inhibition of this pathway by bioactive compounds from *Annona muricata* may have contributed to enhanced renal antioxidant defenses and reduced fibrosis, as PI3K/Akt activation has been implicated in crystal-induced epithelial-mesenchymal transition (EMT) and renal injury (Zhao & Yang, 2023). Research by (Wang et al., 2018) highlighted the involvement of PI3K/Akt in kidney stone disease, particularly in EMT development and calcium oxalate crystal formation in renal tubular epithelial cells (TECs). The study further indicated that silencing the gastrin-releasing peptide receptor (GRPR) gene suppresses EMT and CaOx crystal formation by inactivating PI3K/Akt signaling. Zhao and Yang (2023) expanded on this mechanism, discussing ferroptosis in CaOx kidney stone formation and the ANKRD1 gene's regulatory role, which is also linked to the PI3K/Akt pathway. These interconnected mechanisms suggest that *A. muricata* ethanol extract phytochemicals exert protective effects against CaOx nephrolithiasis by targeting multiple pathways involved in stone formation and prevention.

Molecular docking analysis confirmed strong interactions between *A. muricata* compounds and proinflammatory cytokines TNF- α and IL-1 β (Table 1). Caryophyllene oxide exhibited high-affinity binding to TNF- α (-6.3 kcal/mol), comparable to the standard ligand (-6.8 kcal/mol), reinforcing its reported anti-inflammatory efficacy (Gushiken et al., 2022; Li et al., 2021). Another promising compound, 5,9,13-Pentadecatrien-2-one, 6,10,14-trimethyl-, displayed dual-target binding (-5.3 kcal/mol for TNF- α and -5.8 kcal/mol for IL-1 β), indicating potential broad-spectrum anti-inflammatory properties. Structure-activity relationship analysis revealed sesquiterpenes demonstrated stronger binding interactions than long-chain hydrocarbons ($\Delta G > -4.5$ kcal/mol), consistent with Magalhães et al. (2022), who found that cyclic sesquiterpenes exhibit enhanced binding to inflammatory mediators compared to linear molecules. The robust binding of *A. muricata* metabolites to TNF- α and IL-1 β aligns with antinephrolithiasis potential of the extract, since TNF- α and IL-1 β drive inflammation-induced renal injury (Huang et al., 2024). By neutralizing these cytokines, Caryophyllene oxide and other sesquiterpenes may have mitigated CaOx deposition, renal fibrosis, and nephron obstruction, underpinning the observed therapeutic benefits in vivo.

Pharmacokinetic analysis is essential in assessing drug efficacy. Studies emphasize early ADME (Absorption, Distribution, Metabolism, Excretion) evaluation to reduce development failures (Daina & Zoete, 2019; Ferreira & Andricopulo, 2019). Effective molecular docking profiles must align with pharmacokinetic viability to ensure therapeutic plasma levels and real-world clinical utility. In this study, highly docked compounds like Caryophyllene oxide demonstrated high gastrointestinal absorption, correlating with strong systemic bioavailability following oral administration. Approximately 54.2% of evaluated compounds exhibited high gastrointestinal absorption, correlating with their lipophilicity profiles (Fallon Adido et al., 2023). Lipophilic compounds tend to exhibit enhanced membrane permeability, allowing for efficient intracellular targeting of cytokine receptors and oxidative stress mediators (Kang et al., 2011). The Topological Polar Surface Area (TPSA) values ranged from 0.00 to 115.45 Å², with compounds like Caryophyllene oxide and 2-Methoxy-4-vinylphenol showing blood-brain barrier permeability, highlighting their potential neurological applications (Liu et al., 2023). While BBB penetration is advantageous for neurological treatments, high renal membrane permeability ensures better distribution in kidney tissues, allowing direct modulation of inflammatory and oxidative stress pathways (Du et al., 2018). The acute toxicity assessment of *A. muricata* leaf ethanol extract at a dosage of 6000 mg/kg body weight revealed no treatment-related behavioral changes or mortality in rats within 24 hours observation period, implying an LD₅₀ value exceeding 6000 mg/kg, which is considered safe (Solecki

et al., 2017). The *in-vivo* acute toxicity test observed in this study further justified the *in-silico* ADME test carried out that *A. muricata* ethanol extract is not toxic and can be easily absorbed.

V. Conclusion

This study highlights the promising therapeutic potential of ethanol *Annona muricata* leaf extract in nephrolithiasis management. The phytochemical profiling through GC-MS analysis revealed the presence of bioactive compounds that may contribute to its antioxidant, anti-inflammatory and nephroprotective properties. *In-vitro* assays demonstrated its ability to neutralize free radicals, suggesting a protective effects against oxidative stress a key factor in kidney stone formation. Furthermore, acute toxicity assessment provided evidence of its safety, supporting its potential for medicinal applications. The *in-silico* investigations, including molecular docking and gene ontology analysis, unveiled possible mechanisms underlying *A. muricata* ethanol extract nephron protective efficacy, reinforcing its therapeutic relevance. Overall, the findings support *A. muricata* as a promising natural remedy for nephrolithiasis prevention and management. Future studies involving clinical trials are necessary to validate its efficacy and establish standardized dosing parameters for safe and effective use in medical applications.

ACKNOWLEDGEMENT

We gratefully recognise the contributions made by the study team and the entire laboratory staff of the Department of Biochemistry, Crescent University Abeokuta

Conflict of interest

The authors declare no conflict of interest.

DATA AVAILABILITY

Data produced from this study are available from the corresponding author upon reasonable request.

Ethical Approval

The National Academy of Science's (NAS) "Guide for the Care and Use of Laboratory Animals" (National Research Council, 2010) provided guidelines that all of the animals were treated with care. The institution has approved the researcher's experiment under number CRESCENT/CS/BCH/PG/S41512005 Crescent University Departmental Ethical Committee,

References

- [1]. Aborode, A. T., Awuah, W. A., Mikhailova, T., Abdul-Rahman, T., Pavlock, S., Kundu, M., Yarlagadda, R., Pustake, M., Correia, I. F. d. S., & Mehmood, Q. (2022). OMICs technologies for natural compounds-based drug development. *Current Topics in Medicinal Chemistry*, 22(21), 1751-1765.
- [2]. Adedeji, A. A., Talabi, I. E., & Oladoja, F. (2023). Alternative Medicine in Health Care: Is the Time not Now to Standardize African Phytomedicine to Indigenize Health Care and Create Entrepreneurial Opportunities? In *Medical Entrepreneurship: Trends and Prospects in the Digital Age* (pp. 259-273). Springer.
- [3]. Afolabi, M. O. (2013). A disruptive innovation model for indigenous medicine research: a Nigerian perspective. *African Journal of Science, Technology, Innovation and Development*, 5(6), 445-457.
- [4]. Ajiboye, A., & Olawoyin, R. (2020). Antibacterial activities and phytochemical screening of crude extract of *Carica papaya* leaf against selected pathogens. *Global journal of pure and applied sciences*, 26(2), 165-170.
- [5]. Akinloye, D. I., & Ugboja, R. N. (2022). Potential nutritional benefits of *Ficus exasperata* Vahl leaf extract. *Nutrire*, 47(1), 6.
- [6]. Arcidiacono, T., Mingione, A., Macrina, L., Pivari, F., Soldati, L., & Vezzoli, G. (2015). Idiopathic calcium nephrolithiasis: a review of pathogenic mechanisms in the light of genetic studies. *American journal of nephrology*, 40(6), 499-506.
- [7]. Balogun, J. A. (2022). Emerging developments in traditional medicine practice in Nigeria. In *The Nigerian Healthcare System: Pathway to Universal and High-Quality Health Care* (pp. 235-275). Springer.
- [8]. Butnariu, M., Kumar, M., Calina, D., & Cho, W. C. (2022). A Review of Recent Studies on the Antioxidant and Anti-Infectious Properties of Senna Plants.
- [9]. Chan, G. K., McGrath, J. A., & Parsons, M. (2021). Spatial activation of ezrin by epidermal growth factor receptor and focal adhesion kinase co-ordinates epithelial cell migration. *Open biology*, 11(8), 210166.
- [10]. Cheng, L. P., Huang, X. Y., Wang, Z., Kai, Z. P., & Wu, F. H. (2014). Combined 3D-QSAR, molecular docking, and molecular dynamics study on potent cyclohexene-based influenza neuraminidase inhibitors. *Monatshefte für Chemie-Chemical Monthly*, 145, 1213-1225.
- [11]. Daina, A., & Zoete, V. (2019). Application of the SwissDrugDesign online resources in virtual screening. *International journal of molecular sciences*, 20(18), 4612.
- [12]. de Albuquerque, U. P., de Lima Araujo, E., El-Deir, A. C. A., de Lima, A. L. A., Souto, A., Bezerra, B. M., Ferraz, E. M. N., Maria Xavier Freire, E., Sampaio, E. V. d. S. B., & Las-Casas, F. M. G. (2012). Caatinga revisited: ecology and conservation of an important seasonal dry forest. *The Scientific World Journal*, 2012(1), 205182.
- [13]. Du, S. Q., Wang, X. R., Zhu, W., Ye, Y., Yang, J. W., Ma, S. M., Ji, C. S., & Liu, C. Z. (2018). Acupuncture inhibits TXNIP- associated oxidative stress and inflammation to attenuate cognitive impairment in vascular dementia rats. *CNS neuroscience & therapeutics*, 24(1), 39-46.
- [14]. Fallon Adido, H. E., Silva Chagas, C. K., Ferreira, G. G., Carmo Bastos, M. L., & Dolabela, M. F. (2023). In silico studies on cytotoxicity and antitumoral activity of acetogenins from *Annona muricata* L. *Frontiers in Chemistry*, 11, 1316779.
- [15]. Ferreira, L. L., & Andricopulo, A. D. (2019). ADMET modeling approaches in drug discovery. *Drug discovery today*, 24(5), 1157-1165.
- [16]. Gfeller, D., Grosdidier, A., Wirth, M., Daina, A., Michielin, O., & Zoete, V. (2014). SwissTargetPrediction: a web server for target prediction of bioactive small molecules. *Nucleic acids research*, 42(W1), W32-W38.

- [17]. Gross, O., Girgert, R., Beirowski, B., Kretzler, M., Kang, H. G., Kruegel, J., Miosge, N., Busse, A.-C., Segerer, S., & Vogel, W. F. (2010). Loss of collagen-receptor DDR1 delays renal fibrosis in hereditary type IV collagen disease. *Matrix biology*, 29(5), 346-356.
- [18]. Gushiken, L. F. S., Beserra, F. P., Hussni, M. F., Gonzaga, M. T., Ribeiro, V. P., De Souza, P. F., Campos, J. C. L., Massaro, T. N. C., Hussni, C. A., & Takahira, R. K. (2022). Beta- caryophyllene as an antioxidant, anti- inflammatory and re- epithelialization activities in a rat skin wound excision model. *Oxidative medicine and cellular longevity*, 2022(1), 9004014.
- [19]. Hassan, H., El-Desouky, A. I., Ibrahim, A., El-Kenawy, E.-S. M., & Arnous, R. (2020). Enhanced QoS-based model for trust assessment in cloud computing environment. *Ieee Access*, 8, 43752-43763.
- [20]. Huang, Y., Xu, L., Yang, Q., Xiao, X., Ye, Z., Li, R., Guan, Y., & Wu, X. (2024). NLRP12 c. 1382dup promotes the development of Crohn's disease through the ERK/NLRP3/IL-1 β pathway. *Gene*, 931, 148855.
- [21]. Isaac, I. O., Etesin, U. M., Nya, E. J., Ukpog, E. J., Isotuk, U. G., & Ibok, U. J. (2022). Ethnobotanical study, phytochemical composition and in vitro antioxidant activity of the methanol extracts of thirty-two medicinal plants from Southern Nigeria. *Journal of Medicinal Plants Research*, 16(10), 288-299.
- [22]. Kang, D. H., Lee, D. J., Lee, K. W., Park, Y. S., Lee, J. Y., Lee, S.-H., Koh, Y. J., Koh, G.-Y., Choi, C., & Yu, D.-Y. (2011). Peroxiredoxin II is an essential antioxidant enzyme that prevents the oxidative inactivation of VEGF receptor-2 in vascular endothelial cells. *Molecular cell*, 44(4), 545-558.
- [23]. Kang, Y. G., Jang, H., Park, Y., & Kim, B.-M. (2020). Development of a 3-D physical dynamics monitoring system using OCM with DVC for quantification of sprouting endothelial cells interacting with a collagen matrix. *Materials*, 13(12), 2693.
- [24]. Keramatipour, M., Ahadi, B., Taghizadeh, M., Tabibi, A., Zohrabi, F., Javanmard, B., & Narouie, B. (2018). Investigation of the association of G-7A and T-138C single nucleotide polymorphisms on the promoter of MGP gene with renal stone. *Journal of Nephropharmacology*, 7(2), 145-148.
- [25]. Khan, S. R. (2014). Reactive oxygen species, inflammation and calcium oxalate nephrolithiasis. *Translational andrology and urology*, 3(3), 256.
- [26]. Khanal, S. (2021). Qualitative and quantitative phytochemical screening of Azadirachta indica Juss. plant parts. *International Journal of Applied Sciences and Biotechnology*, 9(2), 122-127.
- [27]. Kumar, K. A., Sharma, M., Dalal, V., Singh, V., Tomar, S., & Kumar, P. (2021). Multifunctional inhibitors of SARS-CoV-2 by MM/PBSA, essential dynamics, and molecular dynamic investigations. *Journal of Molecular Graphics and Modelling*, 107, 107969.
- [28]. Li, H., Prever, L., Hirsch, E., & Gulluni, F. (2021). Targeting PI3K/AKT/mTOR signaling pathway in breast cancer. *Cancers*, 13(14), 3517.
- [29]. Liu, G., Li, Y., Kong, Q., & Tong, H. (2017). Research on ECM process of micro holes with internal features. *Precision Engineering*, 47, 508-515.
- [30]. Liu, Y., Li, H., Huang, R., Li, H., Xu, Y., Li, F., Shen, X., Han, S., & Pan, C. (2023). Differences in Physicochemical properties and flavor components among different layers of medium-temperature Daqu.
- [31]. Magalhães, B. Q., Machado, F. P., Sanches, P. S., Lima, B., Falcão, D. Q., von Ranke, N., Bello, M. L., Rodrigues, C. R., Santos, M. G., & Rocha, L. (2022). Eugenia sulcata (Myrtaceae) nanoemulsion enhances the inhibitory activity of the essential oil on P2X7R and inflammatory response in vivo. *Pharmaceutics*, 14(5), 911.
- [32]. Mao, D., Xu, R., Chen, H., Chen, X., Li, D., Song, S., He, Y., Wei, Z., & Zhang, C. (2021). Cross-talk of focal adhesion-related gene defines prognosis and the immune microenvironment in gastric cancer. *Frontiers in Cell and Developmental Biology*, 9, 716461.
- [33]. McCurdy, S. M., Dai, Q., Zhang, J., Zamilpa, R., Ramirez, T. A., Dayah, T., Nguyen, N., Jin, Y.-F., Bradshaw, A. D., & Lindsey, M. L. (2011). SPARC mediates early extracellular matrix remodeling following myocardial infarction. *American Journal of Physiology-Heart and Circulatory Physiology*, 301(2), H497-H505.
- [34]. Mohamadi-Cheraghbabadi, M., & Hazrati, S. (2023). Terpenoids, steroids, and phenolic compounds of medicinal plants. *Phytochem Med Plants: Biodivers Bioact Drug Discov*, 105-130.
- [35]. Murugesan, A., Kumar, L., & Janarthanan, P. (2018). Status of single nucleotide polymorphism of Matrix Gla protein gene (rs4236) in nephrolithiasis: a preliminary study in Indian population. *International Journal of Applied and Basic Medical Research*, 8(1), 38-41.
- [36]. Mutakin, M., Fauziati, R., Fadhillah, F. N., Zuhrotun, A., Amalia, R., & Hadisaputri, Y. E. (2022). Pharmacological activities of soursop (Annona muricata Lin.). *Molecules*, 27(4), 1201.
- [37]. Nafiu, M. O., & Ogunsola, I. J. (2023). Anti-nephrolithiatic evaluation of partitioned ethanol extract of Calo tropis procera Leaf in wistar rats. *Jordan J Biol Sci*, 16, 105-115.
- [38]. Oefner, C., Sharkey, A., Gardner, L., Critchley, H., Oyen, M., & Moffett, A. (2015). Collagen type IV at the fetal-maternal interface. *Placenta*, 36(1), 59-68.
- [39]. Ogwu, M. C., & Osawaru, M. E. (2022). Traditional methods of plant conservation for sustainable utilization and development. In *Biodiversity in Africa: potentials, threats and conservation* (pp. 451-472). Springer.
- [40]. Olugbuyi, A. O., Oluwajuyitan, T. D., Adebayod, I. N., & Anosike, U. M. (2023). Nutrient, amino acids, phytochemical and antioxidant activities of common Nigeria indigenous soups. *Journal of Agriculture and Food Research*, 11, 100497.
- [41]. Onaran, M., Yilmaz, A., Şen, İ., Ergun, M. A., Çamtosun, A., Küpeli, B., Menevşe, S., & Bozkırlı, İ. (2009). A HindIII polymorphism of fibronectin gene is associated with nephrolithiasis. *Urology*, 74(5), 1004-1007.
- [42]. Pan, Y., Cui, Y., Yu, S., Zhang, Q., Fan, J., Abdul Rasheed, B., & Yang, K. (2014). The expression of epidermal growth factor (EGF) and its receptor (EGFR) during post- natal testes development in the yak. *Reproduction in Domestic Animals*, 49(6), 970-976.
- [43]. Schulz, H., & Georgy, U. (2012). *From CA to CAS online: databases in chemistry*. Springer Science & Business Media.
- [44]. Shahzad, R., Shehzad, A., Bilal, S., & Lee, I.-J. (2020). Bacillus amyloliquefaciens RWL-1 as a new potential strain for augmenting biochemical and nutritional composition of fermented soybean. *Molecules*, 25(10), 2346.
- [45]. Sharma, B., & Albig, A. R. (2013). Matrix Gla protein reinforces angiogenic resolution. *Microvascular research*, 85, 24-33.
- [46]. Shehadeh, M. B., Suaifan, G. A., & Abu-Odeh, A. M. (2021). Plants secondary metabolites as blood glucose-lowering molecules. *Molecules*, 26(14), 4333.
- [47]. Solecki, R., Schumacher, D. M., Pfeil, R., Bhula, R., & MacLachlan, D. J. (2017). OECD Guidance documents and test guidelines. In *Food Safety Assessment of Pesticide Residues* (pp. 13-36). World Scientific.
- [48]. Song, S., Eckerle, S., Onichtchouk, D., Marrs, J. A., Nitschke, R., & Driever, W. (2013). Pou5f1-dependent EGF expression controls E-cadherin endocytosis, cell adhesion, and zebrafish epiboly movements. *Developmental cell*, 24(5), 486-501.
- [49]. Sun, M., Chi, G., Xu, J., Tan, Y., Xu, J., Lv, S., Xu, Z., Xia, Y., Li, L., & Li, Y. (2018). Extracellular matrix stiffness controls osteogenic differentiation of mesenchymal stem cells mediated by integrin $\alpha 5$. *Stem cell research & therapy*, 9, 1-13.

- [50]. Taguchi, T., Kubota, M., Saito, M., Hattori, H., Kimura, T., & Marumo, K. (2016). Quantitative and qualitative change of collagen of Achilles tendons in rats with systemic administration of glucocorticoids. *Foot & Ankle International*, 37(3), 327-333.
- [51]. Tian, Z., Wang, C.-K., Lin, F.-L., Liu, Q., Wang, T., Sung, T.-C., Alarfaj, A. A., Hirad, A. H., Lee, H. H.-C., & Wu, G.-J. (2022). Effect of extracellular matrix proteins on the differentiation of human pluripotent stem cells into mesenchymal stem cells. *Journal of Materials Chemistry B*, 10(30), 5723-5732.
- [52]. Udofia, P. G., Ojmelukwe, P. C., Olaoye, O. A., Ukoma, A. N., Ekanem, M. L., & Okparauka, I. I. (2022). Evaluation of Antioxidant Activity of Ethanol Extract of Root and Stem Bark of Moringa oleifera (MO) obtained from Utu Ikpe, Ikot Ekpene Local Government Area, Nigeria. *Communication in Physical Sciences*, 8(1), 1-8.
- [53]. Ursini, F., Maiorino, M., Morazzoni, P., Roveri, A., & Pifferi, G. (1994). A novel antioxidant flavonoid (IdB 1031) affecting molecular mechanisms of cellular activation. *Free Radical Biology and Medicine*, 16(5), 547-553.
- [54]. Wang, H., Wang, Y., Gao, H., Wang, B., Dou, L., & Li, Y. (2018). Piperlongumine induces apoptosis and autophagy in leukemic cells through targeting the PI3K/Akt/mTOR and p38 signaling pathways. *Oncology Letters*, 15(2), 1423-1428.
- [55]. Wei, B., Jin, C., Xu, Y., Du, X., Yan, C., Tang, C., Ansari, M., & Wang, L. (2014). Chondrogenic differentiation of marrow clots after microfracture with BMSC-derived ECM scaffold in vitro. *Tissue Engineering Part A*, 20(19-20), 2646-2655.
- [56]. Xu, Y., Liang, H., Mao, X., Song, Z., Shen, X., Ge, D., Chen, Y., Hou, B., & Hao, Z. (2024). Puerarin ameliorates apoptosis and inflammation induced by kidney stones through the PI3K/AKT pathway: Network pharmacology and experimental validation.
- [57]. Zhao, Y., & Yang, W. (2023). The effects of hormone-mediated PI3K/AKT signaling on spermatogenesis in Sertoli cells. *Biocell*, 47(8), 1709.